Chemical Science

ROYAL SOCIETY OF CHEMISTRY

EDGE ARTICLE

View Article Online
View Journal | View Issue

Cite this: *Chem. Sci.*, 2025, **16**, 23088

All publication charges for this article have been paid for by the Royal Society of Chemistry

Received 8th September 2025
Accepted 20th October 2025

DOI: 10.1039/d5sc06912b

rsc.li/chemical-science

A methyltransferase molecular switch unlocks *para*-quinone methide generation and oligomerization

Chuanteng Ma,†[ab] Zhenzhen Zhang,†[c] Wenxue Wang,†[ab] Falei Zhang,[a] Aowei Xie,[d] Kaijin Zhang,[a] Xingtao Ren,[a] Lu Wang,[a] Qian Che,[a] Tianjiao Zhu,[a] Junfeng Zhang*[a] and Dehai Li*[ab]

Quinone methides (QMs) are highly reactive intermediates with dual electrophilic/nucleophilic character, serving as versatile synthons in organic synthesis and biosynthesis. Their broader utility remains limited by their inherent instability and scarce practical generation methods. While biosynthetic *o*-QM formation from *ortho*-hydroxybenzyl alcohols is well-established, dedicated pathways to generate *p*-QMs that function as building blocks remain elusive. Here, we report a fungal biosynthetic pathway from *Mycocitrus zonatus* strain Mcr that generates a reactive 2,4-dihydroxybenzyl alcohol precursor. Crucially, a novel family of membrane-dependent methyltransferase (AcreE) acts as a "molecular switch" by masking the *ortho*-hydroxy group, encouraging *p*-QM formation and blocking conventional *o*-QM generation. This *p*-QM undergoes iterative intermolecular 1,6-conjugate additions, yielding oligomeric products. This study reveals a dedicated *p*-QM biosynthetic logic, not only demonstrating methylation as a strategy to control the fate of the reactive intermediate, but also providing novel machinery for accessing synthetically challenging *p*-QM intermediates.

Introduction

Quinone methides (QMs) are important highly reactive intermediates featuring a cross-conjugated quinoid–methylene system, which imparts remarkable electrophilicity and kinetic instability. The distinctive reactivity of QMs drives their widespread application in organic synthesis, enabling diverse C–C and C–O bond-forming transformations to afford complex scaffolds as valuable and versatile synthons.[1,2]

QMs primarily exist in two isomeric forms: *ortho*-quinone methides (*o*-QMs or 1,2-QMs) and *para*-quinone methides (*p*-QMs or 1,4-QMs).[1] Both exhibit dual electrophilic–nucleophilic reactivity due to the partial zwitterionic character, yet their reactivity profiles are fundamentally distinct (Fig. 1A). *o*-QMs have been extensively exploited for constructing complex molecular frameworks, notably *via* [4 + 2] cycloadditions and 1,4-conjugate additions.[3–7] In contrast, *p*-QMs have gained prominence in asymmetric synthesis only within the past decade, primarily through 1,6-conjugate additions.[8,9] However, the high reactivity and inherent instability of QMs have limited their broader utility in organic synthesis. To address this challenge and unlock their synthetic potential, strategies for the one-pot *in situ* generation of QMs have been developed. These approaches enable the direct construction of complex molecular scaffolds, with prominent examples including *o*-QM generation from *ortho*-hydroxybenzyl alcohols and *p*-QM generation from *para*-hydroxybenzyl alcohols (Fig. 1B).[1,10,11]

QMs also serve as key biosynthetic building blocks in the assembly of complex natural products.[12,13] Recent studies have elucidated the biosynthetic logic for *o*-QMs, establishing *ortho*-hydroxybenzyl alcohol derivatives – generated by non-reducing polyketide synthases (nrPKSs) and tailoring enzymes – as direct precursors. These precursors undergo spontaneous or enzyme-catalyzed dehydration to generate the reactive *o*-QM intermediates (Fig. 1C and S1).[14–19] This mechanistic understanding has facilitated the development of enzymatic *o*-QM production methods and inspired strategies to harness these intermediates for constructing pseudo-natural product libraries, thereby expanding structural diversity and advancing the chemical evolution of natural products.[12,20–22] In contrast, the potential of *p*-QMs as versatile synthons for 1,6-conjugate additions remains largely untapped, despite their roles in certain biosynthetic pathways (Fig. S2).[13] This limitation stems

[a]*School of Medicine and Pharmacy, Key Laboratory of Marine Drugs Ministry of Education, Sanya Oceanographic Institute, Frontiers Science Center for Deep Ocean Multispheres and Earth System, Ocean University of China, Qingdao 266000, China. E-mail: jfzhang@ouc.edu.cn; dehaili@ouc.edu.cn*

[b]*Laboratory for Marine Drugs and Bioproducts, Qingdao Marine Science and Technology Center, Qingdao 266237, China*

[c]*School of Medicine, Jiaozuo Key Laboratory for Huaiyao Comprehensive Development, Henan Polytechnic University, Jiaozuo 454000, China*

[d]*College of Food Science and Engineering, Ocean University of China, Qingdao 266404, China*

† These authors contributed equally to this work.

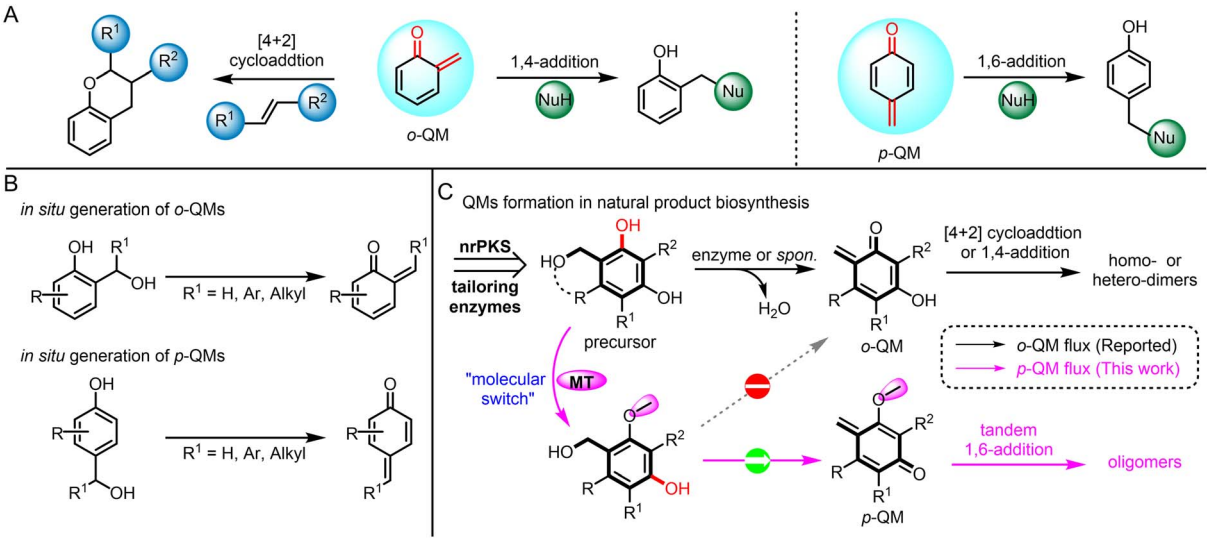

Fig. 1 A) Primary reaction styles of *o*-QMs and *p*-QMs. (B) Methods for *in situ* generation of *o*-QMs and *p*-QMs. (C) Formation of *o*-QMs (reported, black arrow) and *p*-QMs (this work, pink arrow) in natural product biosynthesis. Nu: nucleophile. nrPKS: non-reducing polyketide synthase. MT: methyltransferase.

primarily from two factors: (1) most characterized *p*-QM reactions occur intramolecularly, precluding intermolecular coupling applications; (2) unlike their *ortho* counterparts, readily accessible equivalents enabling direct and controlled generation of *p*-QMs are lacking, as their formation typically requires enzymatic mediation. Consequently, the application of *p*-QMs as versatile molecular building blocks is significantly constrained. Therefore, the discovery of novel routes to *p*-QMs enables substantial expansion of the chemical toolbox for pharmaceutical discovery and complex molecule synthesis.

In this study, through heterologous expression and *in vitro* microsomal assays we identify a readily accessible *p*-QM and reveal a dedicated *p*-QM route from the marine fungus *Mycocitrus zonatus* Mcr. This pathway parallels the canonical *o*-QM logic, employing a nrPKS and a short-chain dehydrogenase/reductase (SDR) to generate a 2,4-dihydroxybenzyl alcohol precursor. Crucially, this precursor possesses dual reactivity potential, enabling formation of either *o*-QM or *p*-QM intermediates. Intriguingly, pathway specificity is dictated by an uncharacterized, membrane-dependent methyltransferase (MT, AcreE) that regioselectively methylates the *ortho*-hydroxy group. This methylation event precludes dehydration at the *ortho* position, effectively blocking *o*-QM formation and exclusively channeling the precursor towards *p*-QM generation. The resulting reactive *p*-QM species then undergoes iterative intermolecular 1,6-conjugate additions, yielding a series of oligomeric products. MT-catalyzed methylation constitutes a pivotal tailoring step in natural product biosynthesis, profoundly altering molecular structure, bioactivity, bioavailability, and ultimately, ecological adaptation.[23,24] Herein, we reveal methylation acting as a molecular switch, directing flux exclusively towards *p*-QM production. This strategy exemplifies how nature exploits a simple methyl modification to exert precise control over the generation of highly reactive intermediates and dictates reaction trajectory. Our findings provide a novel paradigm for understanding and harnessing reactive intermediates in biosynthesis and organic synthesis. Critically, this study highlights that the roles of MTs extend far beyond conventional functionalization, revealing their underappreciated capacity for multifaceted catalytic versatility in orchestrating complex biosynthetic outcomes.

Results and discussion

Structural characterization of acrepolyphenols reveals a *p*-QM-mediated oligomerization pathway. In our systematic investigation of bioactive fungal metabolites, chemical analysis of the marine-derived fungus *Mycocitrus zonatus* Mcr led to the isolation of eleven structurally related polyphenols, all of which are new compounds, determined as acrepolyphenols A–K. (**1–11**, Fig. 2). Comprehensive structural elucidation through HR-MS and NMR analyses (Tables S4–S14, S13–S23 and S27–S81) revealed these compounds as a series of oligomeric derivatives ranging from monomeric to pentameric forms, interconnected through C1–C4′ and/or C1–C6′ linkages. Biological evaluation demonstrated anti-influenza A (H1N1) activity for compounds **1** (IC_{50} = 72 μM) and **7** (IC_{50} = 94 μM), with ribavirin as positive control (IC_{50} = 39 μM).

Structural analysis reveals that the monomer **1** shares a core hydroxybenzyl alcohol scaffold with several established *o*-QM precursors, while oligomers **2–11** exhibit connectivity patterns consistent with Michael-type addition products.[20] These observations strongly support a QM-mediated oligomerization cascade. Intriguingly, the C3–*O*-methylation in **1** precludes *o*-QM formation, implying that oligomerization proceeds through *p*-QMs. In addition, the regiospecific C3–*O*-methylation pattern suggests enzymatic control prior to oligomerization, representing an attractive biosynthetic strategy for controlling the fate of the reactive intermediate.

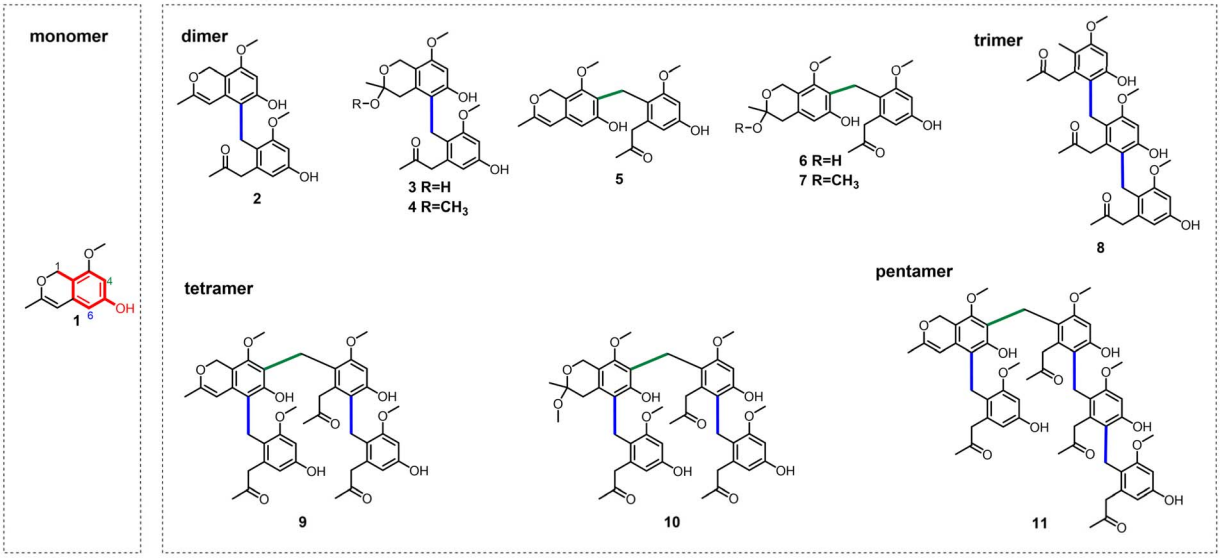

Fig. 2 Structures of acrepolyphenols (**1–11**) isolated from *Mycocitrus zonatus* Mcr. Compounds **3**, **4**, **6**, **7** and **10** were identified as racemic mixtures, respectively. The linkages of C1–C4′ are highlighted in green and C1–C6′ in blue.

A methyltransferase-mediated molecular switch controls *p*-QM formation. Structural characterization of compounds **1–11** suggests a rare *p*-QM intermediate. To understand how the fungus controls *p*-QM production, we investigated the biosynthetic pathway of acrepolyphenols. The genome of the strain *M. zonatus* Mcr was sequenced and analyzed by bioinformatics analysis, revealing an orphan biosynthetic gene cluster (*acre*), which encodes an nrPKS (*acreA*), an SDR (*acreB*), an integral membrane protein (*acreC*), a pathway-specific transcriptional regulator (*acreD*), and a putative methyltransferase (*acreE*) (Fig. 3A, S3 and S4). To ascertain the products of the *acre* gene cluster, we conducted heterologous expression in *Aspergillus nidulans* A1145.[25,26] High performance liquid chromatography (HPLC) analysis of the resulting strain, A1145::*acreABE*, revealed a prominent product peak **12** (Fig. 3B(i and ii)). Notably, **12** exhibited remarkable chemical instability during purification, spontaneously converting to oligomeric derivatives **2–11**. To facilitate structural elucidation, we employed an acetylation strategy using acetic anhydride (Ac_2O)/sodium acetate (NaOAc) treatment of crude extracts, yielding the stabilized derivative **12a**.[27] The acetylated product, **12a**, was isolated and structurally elucidated using NMR (Table S15 and Fig. S82–85). Thus, the structure of **12** was confirmed according to HR-MS ($[M–H]^-$ = 209.0813, Fig. S24) result. Furthermore, we conducted the conversion of extracts from A1145::*acreABE* under various pH conditions (Fig. 3B(iii–vii)). Subsequent pH-dependent stability assays demonstrated that acidic conditions dramatically accelerated oligomerization, while alkaline environments maintained the stability of **12**. This result demonstrates that an acidic environment facilitates the generation of QMs and their subsequent polymerization, consistent with previous reports.[20]

These findings suggest that compound **12** functions as a rare *p*-QM precursor that undergoes stepwise self-oligomerization. In contrast to *o*-QMs, no cycloaddition products of **12** were observed, likely due to the methylation of the hydroxyl group at C3–OH. This site-specific modification suppresses *o*-QM formation, diverting the pathway exclusively toward *p*-QM generation. Consequently, both **12** and its derived *p*-QM (**12′**) participate solely in 1,6-conjugate additions, rendering them incapable of [4 + 2] cycloadditions. Notably, the initial conjugate adducts retain their capacity to regenerate *p*-QMs, enabling iterative oligomerization and ultimately leading to polymeric structures.

Although the *acre* gene cluster has been genetically linked to acrepolyphenol production, the biosynthetic pathway has remained unclear. In order to assign functions to AcreA, AcreB, and AcreE, we first heterologously expressed the nrPKS gene *acreA* in *A. nidulans* A1145, which produced the benzaldehyde precursor **13** (Fig. 3B(viii)). The next enzyme involved in the biosynthesis of **12** is likely to be *acreB* (SDR), whose homologous gene is also present in chaetophenol biosynthetic gene cluster. Co-expression of *acreA* and *acreB* led to the formation of a new compound **14**, although it was unstable for full structural characterization (Fig. 3B(ix)). The HR-MS result indicated a molecular formula of $C_{10}H_{12}O_4$ ($[M–H]^-$ = 195.0658, Fig. S26), **14** Da lower than **13**, suggesting that **14** is a demethylated derivative. It is possible that AcreB catalyzes the reduction of benzaldehyde precursor **13** to yield a benzylic alcohol intermediate, which subsequently undergoes spontaneous hemiacetal cyclization. Notably, the resulting compound **14** bears hydroxy groups at both the *ortho* and *para* positions relative to the benzylic alcohol moiety. This structural feature proves its potential to generate both *o*-QM and *p*-QM intermediates. Subsequently, the remaining unassigned protein AcreE may catalyze the last regioselective methylation, completing the biosynthesis of **12** and directing the reaction pathway exclusively toward *p*-QM generation by blocking the alternative *o*-QM formation route (Fig. 3C).

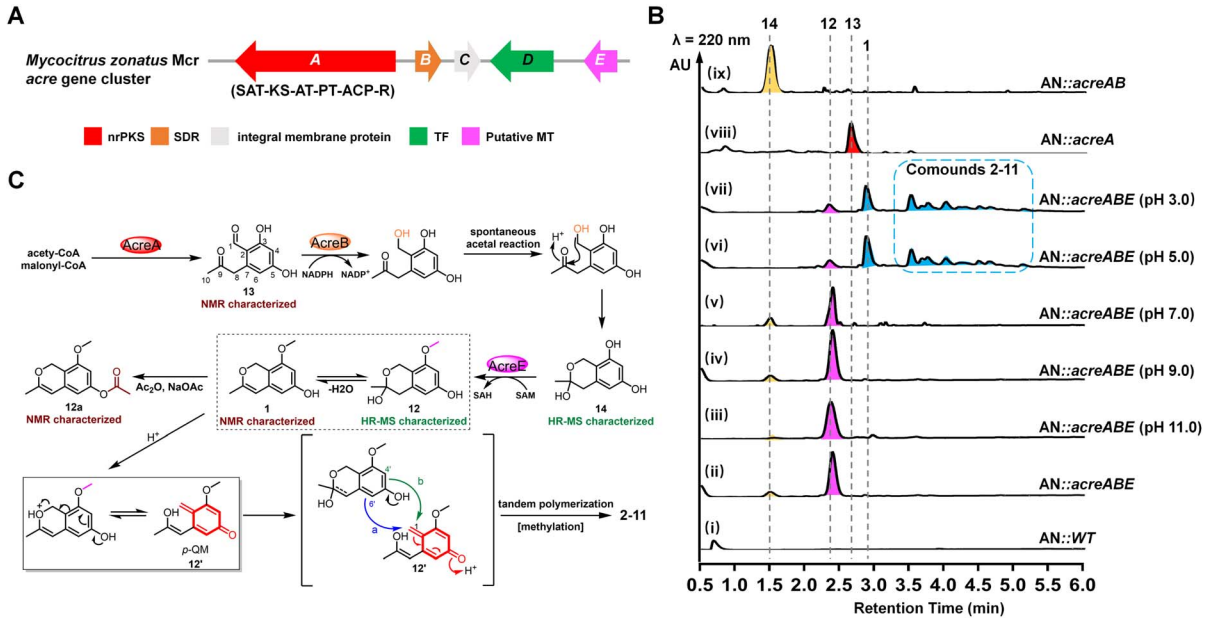

Fig. 3 (A) Organization and proposed function of *acre* gene cluster. (B) HPLC profiles of *A. nidulans* A1145 strain expressing the *acre* gene cluster. (C) Proposed biosynthetic pathway of acrepolyphenols. SAT: starter-unit acyltransferase, KS: ketosynthase, AT: malonyl-CoA:ACP transacylase, PT: product template, ACP: acyl-carrier protein domain, R: reductase.

Functional characterization of AcreE as a novel membrane-dependent methyltransferase. To elucidate the catalytic role of AcreE, we performed comprehensive bioinformatic and functional analyses. AcreE is a 284-residue protein that has no predicted function and conserved domain from the primary sequence (Fig. S6A). Strikingly, Phyre²-based structural homology modeling unveiled sequence identity to SAM-dependent O-MT (Fig. S6B), while SWISS-MODEL analysis demonstrated 79.23% structural similarity (96% coverage) to an uncharacterized MT (AF-A0A1V1SZA7-F1, AlphaFold DB) (Fig. S6C).[28,29] These computational insights prompted us to hypothesize its methyltransferase functionality, despite phylogenetic evidence positioning it outside canonical clades of characterized biosynthetic MTs (Fig. S7). Further analysis indicated that AcreE is a membrane-dependent protein with two continuous transmembrane helices spanning residues 185–207 and 212–234 (Fig. S8). To verify this, the fusion protein with the C-terminus attached to a green fluorescent protein (GFP), AcreE-GFP, was constructed and expressed in *Saccharomyces cerevisiae* BJ5464. Then the microsomal fraction containing membrane protein was extracted from the cytoplasm. We observed GFP fluorescence predominantly in the microsomal fraction, confirming the membrane localization (Fig. S9). We then used yeast microsomal fraction containing AcreE to confirm the function *in vitro*. Given the instability of the proposed substrate (**14**), to verify the function of AcreE, we instead incubated AcreE-containing microsomes with crude extracts from AN::*acreAB*. When the crude was incubated with the microsome containing AcreE or AcreE-GFP, we observed the formation of **12** by comparison with the control (Fig. 4A(i–vii)). The reaction efficiency increased with exogenous SAM, while the supernatant (lacking membrane-bound AcreE) showed weak catalytic activity, likely due to residual microsomal contamination.

SAM-dependent MTs typically contain a conserved GxGxG motif for binding SAM.[23,24] Through multiple sequence alignment of AcreE homologs, we identified two highly conserved motifs: a glycine-rich Motif I CAG(A/G)GGP and a functionally uncharacterized Motif II (C/S)FHHFDD (Fig. S10). Both motifs show remarkable conservation across AcreE-like MTs, suggesting their critical importance in enzymatic function. Structural prediction using AlphaFold confirmed that AcreE adopts a classical Rossmann fold composed of seven β-strands (β1–β7) flanked by α-helices (Fig. S11A). Notably, Motif I is precisely positioned at the C-terminus of β1, while Motif II forms an extended loop bordering β4, collectively constituting the catalytic spatial framework. Detailed structural comparison of the AcreE model with the crystallized 1,6-didemethyltoxoflavin-N1-methyltransferase from *Burkholderia thailandensis* (BthII1283, PDB ID:5UFM) reveals divergent global architecture (RMSD = 11.281 Å over 203 Cα pairs) yet striking preserved catalytic geometry within the catalytic Rossmann fold core (RMSD = 1.394 Å over 48 Cα pairs) (Fig. S11B).[30] Furthermore, AcreE uniquely harbors a transmembrane region featuring dual anti-parallel α-helices connected by a β-hairpin, which is absent in soluble MTs like BthII1283.

Subsequently, we performed the molecular docking of the predicted structure with SAM and substrate **14**, showing that SAM and **14** occupy the cofactor binding pocket and substrate binding pocket of AcreE, respectively (Fig. S12). Interestingly, the transmembrane region covers the methyl receptor binding pocket. This unique membrane-anchoring architecture may potentially establish a hydrophobic conduit enabling vectorial substrate channeling from lipid bilayers to the catalytic

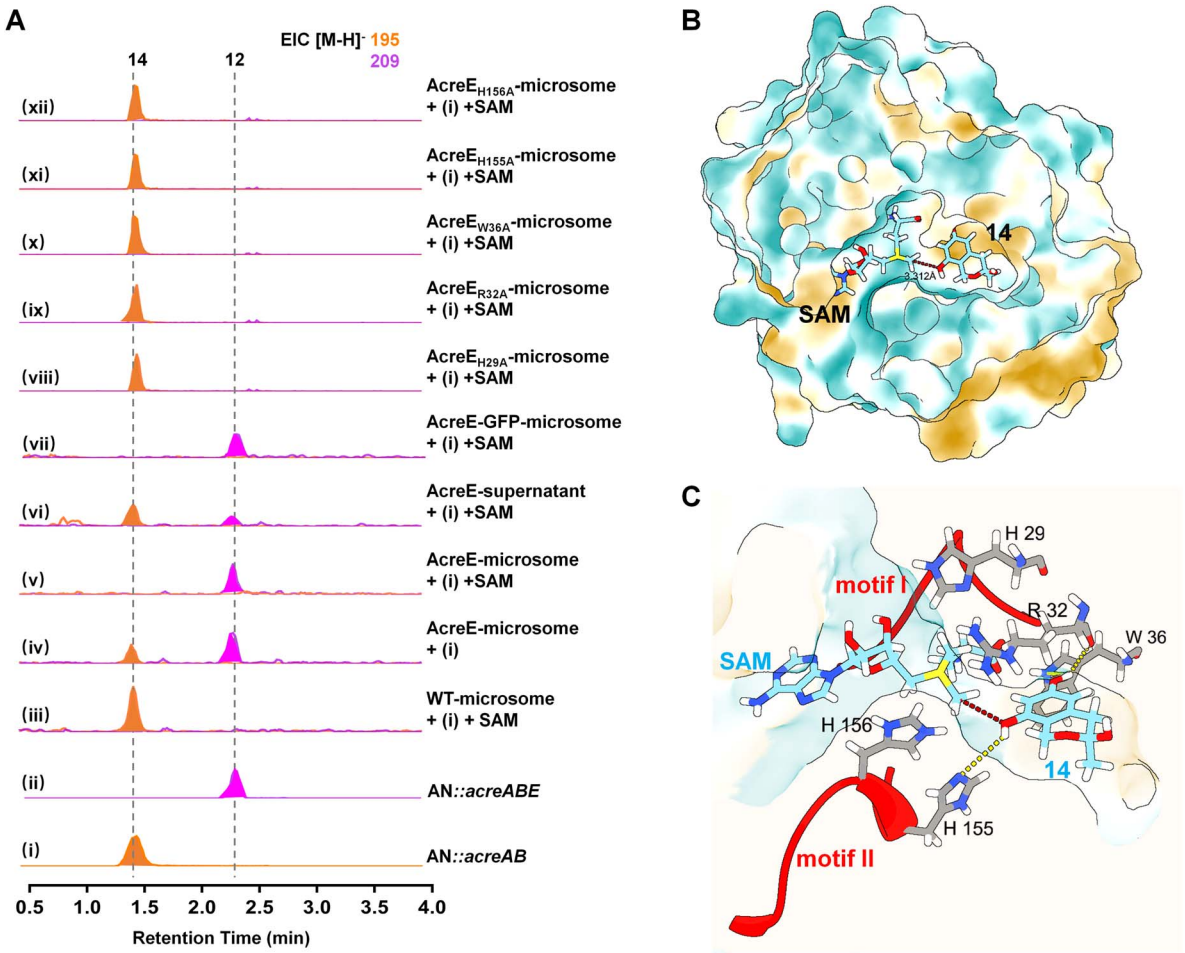

Fig. 4 Functional characterization of AcreE. (A) *In vitro* microsomal assays demonstrate that AcreE functions as a SAM- and membrane-dependent methyltransferase. (B) Computational molecular docking reveals the binding poses of SAM and substrate **14** within the AcreE active site. (C) Schematic model illustrating synergistic interactions between SAM, substrate **14**, and catalytic residues in the AcreE binding pocket. The protein is presented in surface representation, while SAM and compound **14** are displayed as stick models. Motif I and Motif II are labeled in red.

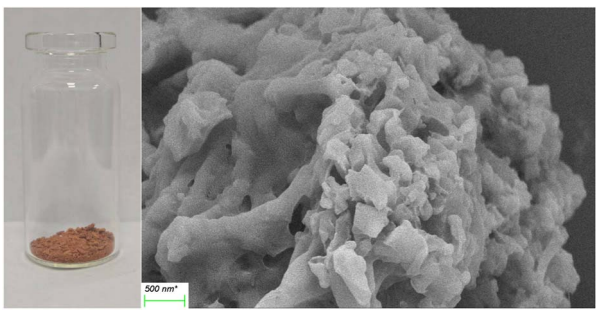

Fig. 5 SEM analysis showing the morphology of the spontaneously polymerized material from *p*-QM monomer **12**.

Rossmann fold and spatiotemporally controlled biosynthesis through compartmentalization of reactive intermediates. Detailed analysis demonstrated that the methyl group of SAM is optimally positioned (3.312 Å) for transferring to the C3–OH of **14** (Fig. 4B). This close proximity strongly supports the observed regiospecific methylation activity. Structural analysis revealed that Motif I and Motif II cooperatively stabilize SAM through distinct interactions: glycine-rich Motif I engages the carboxypropyl moiety while Motif II anchors the sulfonium cation end (Fig. 4C). This arrangement suggests that both motifs are essential for proper SAM orientation. Notably, H29, R32, and W36 from the first α-helix, along with H156 in Motif II, interact with SAM's sulfonium center, likely facilitating methyl transfer, while R32 and W36 additionally hydrogen-bond with substrate **14** to ensure proper positioning. H155 in Motif II appears to function as a general base, activating the C3-hydroxyl through deprotonation for nucleophilic attack on SAM. Functional studies with alanine mutants (H29A, R32A, W36A, H155A, H156A) confirmed the essential role of each residue, as all mutations completely abolished the activity (Fig. 4A(viii–xii)). Collectively, these findings establish AcreE as a membrane-bound SAM-dependent MT that performs the regiospecific methylation at C3–OH of **14**.

MTs are generally soluble cytoplasmic enzymes that catalyze methylation modifications of diverse small molecules and biomacromolecules. While membrane-dependent MTs are

relatively rare, several identified examples play crucial roles in key physiological processes. These include enzymes involved in ubiquinone biosynthesis (*e.g.*, COQ3, COQ5),[31–33] mammalian catechol metabolism and regulation (*e.g.*, transmembrane *O*-methyltransferase, TOMT),[34] and sphingolipid biosynthesis (*e.g.*, sphingolipid C9-methyltransferase, C9MT).[35] Such transmembrane or membrane-anchored MTs typically function by associating with other membrane proteins to form complexes. Their localization enables them to catalyze substrates embedded within the hydrophobic membrane core or positioned on the membrane surface. This spatial organization enhances catalytic efficiency and ensures spatiotemporal specificity. Despite their established roles in primary metabolism, membrane-associated methyltransferases have not been previously identified within natural product biosynthetic pathways. Here, we report the first discovery of a natural product biosynthetic MT harboring a dual-helical transmembrane region. However, the inability to obtain its crystal structure precludes a precise elucidation of the functional role of the transmembrane region in AcreE, necessitating further investigation.

p-QM monomer **12** is a highly promising precursor for functional polymers. Monomer **12** exhibits significant potential as a bio-based building block due to its ability to undergo spontaneous and continuous 1,6-conjugate addition under acidic conditions. This unique characteristic facilitates highly efficient polymerization without requiring additional initiators. To evaluate the viability of compound **12** as a polymerizable monomer, a concentrated solution containing **12** was treated with 0.1% (v/v) formic acid and allowed to stand at room temperature for 7 days. This process yielded a light brown powder and subsequent scanning electron microscopy (SEM) analysis revealed a lamellar porous structure, presumably formed by the stacking of multiple polymer molecules (Fig. 5). This inherent porosity suggests promising utility in biomedical applications, tissue engineering scaffolds, and biotechnological platforms, warranting further development as a sustainable bio-based material or monomer.

Conclusions

In conclusion, this study elucidates a fungal biosynthetic pathway for *p*-QM generation through the discovery and characterization of the *acre* gene cluster from *M. zonatus* Mcr. Structural and functional analyses revealed that the nrPKS (AcreA) and SDR (AcreB) collaboratively synthesize a benzyl alcohol intermediate, while a novel membrane-dependent MT AcreE regio-selectively installs a methyl group that acts as a "biochemical switch" to suppress *o*-QM formation and enforce *p*-QM generation. The discovery of the protective methylation strategy not only reveals Nature's solution to controlling reactive intermediates but also offers a paradigm for bioinspired synthetic methodologies. Furthermore, our work underscores the untapped potential of fungal biosynthetic machinery in generating structurally diverse oligomers through *p*-QM-mediated cascades, highlighting *p*-QM as a unique biosynthetic building block for structural diversification. Significantly, the observed spontaneous polymerization suggests *p*-QMs' potential as bio-based monomers, meriting further material characterization.

Author contributions

C. Ma: conceptualization, methodology, formal analysis, data curation, investigation, visualization, writing – original draft; Z. Zhang: investigation, formal analysis, resources, data curation; W. Wang: investigation, formal analysis, data curation; F. Zhang: formal analysis, data curation, resources; A. Xie: investigation, data curation, resources; K. Zhang: formal analysis, resources; X. Ren: formal analysis, resources; L. Wang: formal analysis; Q. Che: resources, supervision, funding acquisition; T. Zhu: resources, supervision, funding acquisition; J. Zhang: conceptualization, supervision, project administration, funding acquisition; D. Li: conceptualization, supervision, project administration, funding acquisition. C. Ma, Z. Zhang, and W. Wang contributed equally to this work.

Conflicts of interest

The authors declare no conflict of interest.

Data availability

The data supporting this article have been included as part of the supplementary information (SI). Supplementary information: experimental procedures, NMR data, and amino acid sequences. See DOI: **https://doi.org/10.1039/d5sc06912b**.

Acknowledgements

This work was funded by the National Key R&D Program of China (2024YFC2816004), Qingdao Marine Science and Technology Center (2022QNLM030003-1), the Key R&D Program of Hainan Province (ZDYF2023SHFZ144), the Fundamental Research Funds for the Central Universities (202172002, 202172009, and 202262015), the National Natural Science Foundation of China (22207030) and Taishan Scholar Distinguished Expert Program in Shandong Province (tstp20240504). The authors thank Prof. Yi Tang (UCLA, The United States of America) for providing heterologous expression hosts and expression vectors. The authors also thank Prof. Yi Zou (Southwestern University, China) for the assistance in the experiment and Prof. Yu Tang (Ocean University of China) for discussing the results.

References

1 L. Caruana, M. Fochi and L. Bernardi, *Molecules*, 2015, **20**, 11733–11764.
2 K. Ali, P. Mishra, A. Kumar, D. N. Reddy, S. Chowdhury and G. Panda, *Chem. Commun.*, 2022, **58**, 6160–6175.
3 M. S. Singh, A. Nagaraju, N. Anand and S. Chowdhury, *RSC Adv.*, 2014, **4**, 55924–55959.
4 R. S. Lewis, C. J. Garza, A. T. Dang, T. K. A. Pedro and W. J. Chain, *Org. Lett.*, 2015, **17**, 2278–2281.

5 Y. Xie and B. List, *Angew. Chem., Int. Ed.*, 2017, **56**, 4936–4940.
6 B. Yang and S. Gao, *Chem. Soc. Rev.*, 2018, **47**, 7926–7953.
7 M. Uyanik, K. Nishioka, R. Kondo and K. Ishihara, *Nat. Chem.*, 2020, **12**, 353–362.
8 C. G. S. Lima, F. P. Pauli, D. C. S. Costa, A. S. De Souza, L. S. M. Forezi, V. F. Ferreira and F. De Carvalho Da Silva, *Eur. J. Org Chem.*, 2020, **2020**, 2650–2692.
9 J.-Y. Wang, W.-J. Hao, S.-J. Tu and B. Jiang, *Org. Chem. Front.*, 2020, **7**, 1743–1778.
10 M. S. Singh, A. Nagaraju, N. Anand and S. Chowdhury, *RSC Adv.*, 2014, **4**, 55924–55959.
11 C. G. S. Lima, F. P. Pauli, D. C. S. Costa, A. S. De Souza, L. S. M. Forezi, V. F. Ferreira and F. De Carvalho Da Silva, *Eur. J. Org Chem.*, 2020, **2020**, 2650–2692.
12 T. N. Purdy, B. S. Moore and A. L. Lukowski, *J. Nat. Prod.*, 2022, **85**, 688–701.
13 J. Gao, Q. Chen and Q. Zhang, *Nat. Prod. Rep.*, 2025, **42**, 1676–1689.
14 T. Asai, T. Yamamoto, N. Shirata, T. Taniguchi, K. Monde, I. Fujii, K. Gomi and Y. Oshima, *Org. Lett.*, 2013, **15**, 3346–3349.
15 R. Schor, C. Schotte, D. Wibberg, J. Kalinowski and R. J. Cox, *Nat. Commun.*, 2018, **9**, 1963.
16 J. Fan, G. Liao, F. Kindinger, L. Ludwig-Radtke, W.-B. Yin and S.-M. Li, *J. Am. Chem. Soc.*, 2019, **141**, 4225–4229.
17 Q. Chen, J. Gao, C. Jamieson, J. Liu, M. Ohashi, J. Bai, D. Yan, B. Liu, Y. Che, Y. Wang, K. N. Houk and Y. Hu, *J. Am. Chem. Soc.*, 2019, **141**, 14052–14056.
18 X.-X. Wang, B.-Q. Deng, Z.-Q. Ouyang, Y. Yan, J.-M. Lv, S.-Y. Qin, D. Hu, G.-D. Chen, X.-S. Yao and H. Gao, *J. Nat. Prod.*, 2024, **87**, 2139–2147.
19 S. Ren, Y. Yan, Y. Zhou, Y. Han, S. Yuan, J. Chen, H. Guo, Z. Lin, Q. Lin, S. Chen, L. Liu, Y. Qiao and Z. Gao, *Bioorg. Chem.*, 2025, **154**, 108081.
20 T. Asai, K. Tsukada, S. Ise, N. Shirata, M. Hashimoto, I. Fujii, K. Gomi, K. Nakagawara, E. N. Kodama and Y. Oshima, *Nature Chem*, 2015, **7**, 737–743.
21 L.-N. Gao, K. Zheng, H.-Y. Chen, Y.-N. Gao, Z.-Z. Li, C. He, S.-H. Huang, R. Hong, M. Bian and Z.-J. Liu, *Org. Biomol. Chem.*, 2025, **23**, 2775–2792.
22 Y. Wang, D. Li, H. Long, F. Liu, G. Bai, K. Xu and X. Yu, *Org. Biomol. Chem.*, 2025, **23**, 7206–7210.
23 D. K. Liscombe, G. V. Louie and J. P. Noel, *Nat. Prod. Rep.*, 2012, **29**, 1238–1250.
24 E. Abdelraheem, B. Thair, R. F. Varela, E. Jockmann, D. Popadić, H. C. Hailes, J. M. Ward, A. M. Iribarren, E. S. Lewkowicz, J. N. Andexer, P.-L. Hagedoorn and U. Hanefeld, *ChemBioChem*, 2022, **23**, e202200212.
25 T. Nayak, E. Szewczyk, C. E. Oakley, A. Osmani, L. Ukil, S. L. Murray, M. J. Hynes, S. A. Osmani and B. R. Oakley, *Genetics*, 2006, **172**, 1557–1566.
26 D. A. Yee and Y. Tang, in *Engineering Natural Product Biosynthesis*, ed. E. Skellam, Springer US, New York, NY, 2022, vol. 2489, pp. 41–52.
27 M. M. Mojtahedi and S. Samadian, *J. Chem.*, 2013, **2013**, 642479.
28 J. Jumper, R. Evans, A. Pritzel, T. Green, M. Figurnov, O. Ronneberger, K. Tunyasuvunakool, R. Bates, A. Žídek, A. Potapenko, A. Bridgland, C. Meyer, S. A. A. Kohl, A. J. Ballard, A. Cowie, B. Romera-Paredes, S. Nikolov, R. Jain, J. Adler, T. Back, S. Petersen, D. Reiman, E. Clancy, M. Zielinski, M. Steinegger, M. Pacholska, T. Berghammer, S. Bodenstein, D. Silver, O. Vinyals, A. W. Senior, K. Kavukcuoglu, P. Kohli and D. Hassabis, *Nature*, 2021, **596**, 583–589.
29 M. Varadi, D. Bertoni, P. Magana, U. Paramval, I. Pidruchna, M. Radhakrishnan, M. Tsenkov, S. Nair, M. Mirdita, J. Yeo, O. Kovalevskiy, K. Tunyasuvunakool, A. Laydon, A. Žídek, H. Tomlinson, D. Hariharan, J. Abrahamson, T. Green, J. Jumper, E. Birney, M. Steinegger, D. Hassabis and S. Velankar, *Nucleic Acids Res.*, 2024, **52**, D368–D375.
30 M. K. Fenwick, K. H. Almabruk, S. E. Ealick, T. P. Begley and B. Philmus, *Biochemistry*, 2017, **56**, 3934–3944.
31 C. R. Nicoll, L. Alvigini, A. Gottinger, D. Cecchini, B. Mannucci, F. Corana, M. L. Mascotti and A. Mattevi, *Nat. Catal.*, 2024, **7**, 148–160.
32 Y. Zhu, B. Wu, X. Zhang, X. Fan, L. Niu, X. Li, J. Wang and M. Teng, *Biochem. J.*, 2015, **470**, 105–114.
33 Y.-N. Dai, K. Zhou, D.-D. Cao, Y.-L. Jiang, F. Meng, C.-B. Chi, Y.-M. Ren, Y. Chen and C.-Z. Zhou, *Acta Cryst D*, 2014, **70**, 2085–2092.
34 C. Chakraborty, S. Pal, C. G. P. Doss, Z.-H. Wen and C.-S. Lin, *Appl. Biochem. Biotechnol.*, 2012, **167**, 845–860.
35 P. Ternes, P. Sperling, S. Albrecht, S. Franke, J. M. Cregg, D. Warnecke and E. Heinz, *J. Biol. Chem.*, 2006, **281**, 5582–5592.